

A DISCONTINUOUS LEAST SQUARES FINITE ELEMENT METHOD FOR TIME-HARMONIC MAXWELL EQUATIONS

RUO LI, QICHENG LIU, AND FANYI YANG

ABSTRACT. We propose and analyze a discontinuous least squares finite element method for solving the indefinite time-harmonic Maxwell equations. The scheme is based on the L^2 norm least squares functional with the weak imposition of the continuity across the interior faces. We minimize the functional over the piecewise polynomial spaces to seek numerical solutions. The method is shown to be stable without any constraint on the mesh size. We prove the convergence orders under both the energy norm and the L^2 norm. Numerical results in two and three dimensions are presented to verify the error estimates.

keywords: Time-harmonic Maxwell's equations, Least squares method, Discontinuous elements.

1. INTRODUCTION

The time-harmonic Maxwell equations are often encountered in many engineering applications such as antenna design, microwaves, and satellites [13, 29]. These applications require us to carry out numerical studies of the time-harmonic Maxwell equations. The Maxwell's operator is strongly indefinite especially for the case of the high wave number, which brings many difficulties in the numerical simulation and the error analysis [25]. Despite these difficulties, there are plenty of studies on numerical methods for this problem, such as finite difference methods, spectral methods, and finite element methods.

There are a variety of finite element methods for solving the time-harmonic Maxwell equations and related problems. A common choice is to employ the $H(\text{curl})$ -conforming elements, known as edge elements. We refer to [28, 27, 26, 13, 11, 19] for more details of these conforming methods. We note that the implementation of edge elements is still challenging especially in the higher-order case [7].

Using discontinuous functions to approximate the solution, the discontinuous Galerkin (DG) methods have been applied in the numerical simulation of the Maxwell equations. The DG methods can offer great flexibility in the mesh structure which allows the elements of different shapes and can easily handle the irregular non-conforming meshes. Additionally, the implementation of discontinuous elements is very straightforward and there is no need to use the curl-conforming elemental mappings [25]. We refer to [25, 12, 15, 32, 29, 9, 30, 31, 10] and the references therein for those DG methods.

The least squares finite element method (LSFEM) is a general technique in numerical PDEs which is based on the minimization of the L^2 norm of the residual over an approximation space, and we refer to the paper [6] for an overview. The LSFEM has also been applied to solve the Maxwell system and we refer to [7, 8, 18, 16, 17] for such least squares methods. One of the advantages of LSFEM is that the resulting linear system is always

symmetric and positive definite. Recently, the LSFEM has been extended for the numerical approximation to some classical PDEs using discontinuous elements, and this method is referred to as the discontinuous LSFEM. We refer the readers to [2, 3, 5, 4, 23, 24] for more details.

Noticing that the Maxwell's operator is indefinite while the LSFEM always provides a positive definite linear system, we are motivated to develop a stable numerical method, based on the least squares functional and discontinuous elements, to solve the time-harmonic Maxwell equations. For this purpose, we define an L^2 norm least squares functional involving the proper penalty terms which weakly enforce the tangential continuity across the interior faces as well as the boundary conditions. The functional is then minimized over the discontinuous piecewise polynomial spaces to seek the numerical solutions. The method is easy to be implemented and the resulting linear system is shown to be symmetric and positive definite. The method combines the attractive features of DG methods and LSFEMs, giving us a new discontinuous least squares finite element method for the time-harmonic Maxwell equations.

We estimate the error of the new method to derive the convergence rates for all solution variables under both the L^2 norms and the energy norms. It is interesting that the proposed method is shown to be unconditionally stable without making any assumptions about the mesh size. We carry out a series of numerical tests in two and three dimensions to verify the theoretical predictions. Noticing that the least squares functional can serve as an *a posteriori* estimator, we particularly present a low-regularity example, which is solved by the h -adaptive refinement strategy using the least squares functional as an adaptive indicator.

The rest of this paper is organized as follows. In Section 2, we introduce the notations and define the first-order system to the time-harmonic Maxwell equations. In Section 3, we present our least squares method and define the least squares functional. The error estimates are also proven in this section. In Section 4, we present a series of numerical examples to illustrate the accuracy of the proposed method.

2. PRELIMINARIES

Let Ω be an open, bounded polygonal (polyhedral) domain with the boundary $\partial\Omega$ in \mathbb{R}^d , $d = 2, 3$. We denote by \mathcal{T}_h a regular and shape-regular partition over the domain Ω into triangles (tetrahedrons). We let \mathcal{F}_h^i be the collection of all $d - 1$ dimensional interior faces with respect to the partition \mathcal{T}_h , and we let \mathcal{F}_h^b be the collection of all $d - 1$ dimensional faces that are on the boundary $\partial\Omega$, and then we set $\mathcal{F}_h := \mathcal{F}_h^i \cup \mathcal{F}_h^b$. In particular, for the three-dimensional case we denote by \mathcal{E}_h^i the set of all $d - 2$ dimensional interior edges of all elements in \mathcal{T}_h , and by \mathcal{E}_h^b the set of all $d - 2$ dimensional boundary edges, and we let $\mathcal{E}_h := \mathcal{E}_h^i \cup \mathcal{E}_h^b$. For the element $K \in \mathcal{T}_h$ and the face $f \in \mathcal{F}_h$, we let h_K and h_f be their diameters, respectively, and we denote $h := \max_{K \in \mathcal{T}_h} h_K$ as the mesh size of \mathcal{T}_h . Then, the shape-regularity of \mathcal{T}_h is in the sense of that there exists a constant $C > 0$ such that for any element $K \in \mathcal{T}_h$,

$$\frac{h_K}{\rho_K} \leq C,$$

where ρ_K denotes the diameter of the largest disk (ball) inscribed in K .

Next, we introduce the following trace operators that are commonly used in the DG framework. Let $f \in \mathcal{F}_h^i$ be an interior face shared by two adjacent elements K^+ and K^- with the unit outward normal vectors \mathbf{n}^+ and \mathbf{n}^- on f , respectively. For the piecewise smooth scalar-valued function v and the piecewise smooth vector-valued function \mathbf{q} , we define the jump operator $[[\cdot]]$ on f as

$$[[\mathbf{n} \times v]] := \mathbf{n}^+ \times v|_{K^+} + \mathbf{n}^- \times v|_{K^-}, \quad [[\mathbf{n} \times \mathbf{q}]] := \mathbf{n}^+ \times \mathbf{q}|_{K^+} + \mathbf{n}^- \times \mathbf{q}|_{K^-}.$$

For a boundary face $f \in \mathcal{F}_h^b$, we let $K \in \mathcal{T}_h$ be the element that contains f and the jump operator $[[\cdot]]$ on f is defined as

$$[[v]] := \mathbf{n} \times v|_K, \quad [[\mathbf{n} \times \mathbf{q}]] := \mathbf{n} \times \mathbf{q}|_K,$$

where \mathbf{n} is the unit outward normal on f .

We note that the capital C with or without subscripts are generic positive constants, which are possibly different from line to line, are independent of the mesh size h but may depend on the wave number k and the domain Ω . Given a bounded domain $D \subset \Omega$, we will follow the standard notations for the Sobolev spaces $L^2(D)$, $L^2(D)^d$, $H^r(D)$ and $H^r(D)^d$ with the regular exponent $r \geq 0$. We also use the standard definitions of their corresponding inner products, semi-norms and norms. Throughout the paper, we mainly use the notation for the three-dimensional case. For the case $d = 2$, it is natural to identify the space \mathbb{R}^2 with the (x, y) plane in \mathbb{R}^3 . Specifically, in two dimensions for the vector-valued function $\mathbf{u} = (u_1, u_2)^T$, the curl of \mathbf{u} reads

$$\nabla \times \mathbf{u} = \frac{\partial u_2}{\partial x} - \frac{\partial u_1}{\partial y},$$

and for the scalar-valued function q , we let $\nabla \times q$ be the formal adjoint, which reads

$$\nabla \times q = \left(\frac{\partial q}{\partial y}, -\frac{\partial q}{\partial x} \right)^T.$$

For the problem domain Ω , we define the space

$$\begin{aligned} H(\text{curl}) &:= \begin{cases} \{v \in L^2(\Omega) \mid \nabla \times v \in L^2(\Omega)^2\}, & \text{for scalar-valued functions,} \\ \{\mathbf{v} \in L^2(\Omega)^2 \mid \nabla \times \mathbf{v} \in L^2(\Omega)\}, & \text{for vector-valued functions,} \end{cases} & d = 2, \\ H(\text{curl}) &:= \{\mathbf{v} \in L^2(\Omega)^3 \mid \nabla \times \mathbf{v} \in L^2(\Omega)^3\}, & d = 3. \end{aligned}$$

Further, we denote by $H_0(\text{curl})$ the space of functions in $H(\text{curl})$ with vanishing tangential trace,

$$H_0(\text{curl}) := \{\mathbf{v} \in H(\text{curl}) \mid \mathbf{n} \times \mathbf{v} = 0, \text{ on } \partial\Omega\}.$$

For the partition \mathcal{T}_h , we will use the notations and the definitions for the broken Sobolev space $L^2(\mathcal{T}_h)$, $L^2(\mathcal{T}_h)^d$, $H^r(\mathcal{T}_h)$ and $H^r(\mathcal{T}_h)^d$ with the exponent $r \geq 0$ and their associated inner products and norms [1].

The problem under our consideration is to find a numerical approximation to the time-harmonic Maxwell equations in a lossless medium with an inhomogeneous boundary condition, which seeks the electric field $\mathbf{u}(\mathbf{x})$ such that

$$(1) \quad \begin{aligned} \nabla \times \mu_r^{-1} \nabla \times \mathbf{u} - k^2 \varepsilon_r \mathbf{u} &= \mathbf{f}, & \text{in } \Omega, \\ \mathbf{n} \times \mathbf{u} &= \mathbf{g}, & \text{on } \partial\Omega. \end{aligned}$$

Here $\mathbf{f} \in L^2(\Omega)^d$ is an external source file and $k > 0$ is the wave number with the assumption k is not an eigenvalue of the Maxwell system [21, 26, 14]. μ_r and ε_r are the relative magnetic permeability and the relative electric permittivity of the medium. For simplicity, we set $\mu_r = 1$ and $\varepsilon_r = 1$.

Below let us propose a least squares method for the equations (1) based on the discontinuous approximation. We first introduce an auxiliary variable $\mathbf{p} = \frac{1}{k}\nabla \times \mathbf{u}$ to rewrite the Maxwell equations 1 into an equivalent first-order system:

$$(2) \quad \begin{aligned} \nabla \times \mathbf{p} - k\mathbf{u} &= \tilde{\mathbf{f}}, & \text{in } \Omega, \\ \nabla \times \mathbf{u} - k\mathbf{p} &= \mathbf{0}, & \text{in } \Omega, \\ \mathbf{n} \times \mathbf{u} &= \mathbf{g} & \text{on } \partial\Omega, \end{aligned}$$

where $\tilde{\mathbf{f}} = \frac{1}{k}\mathbf{f}$. We note that to rewrite the problem into a first-order system is the fundamental idea in the modern least squares finite element method [6], and our discontinuous least squares method is then based on the system (2).

3. DISCONTINUOUS LEAST SQUARES METHOD FOR TIME-HARMONIC EQUATIONS

Aiming to construct a discontinuous least squares finite element method for (2), we first define a least squares functional based on (2), which reads:

$$(3) \quad \begin{aligned} J_h(\mathbf{u}, \mathbf{p}) &:= \sum_{K \in \mathcal{T}_h} \left(\|\nabla \times \mathbf{p} - k\mathbf{u} - \tilde{\mathbf{f}}\|_{L^2(K)}^2 + \|\nabla \times \mathbf{u} - k\mathbf{p}\|_{L^2(K)}^2 \right) \\ &+ \sum_{f \in \mathcal{F}_h^i} \frac{\mu}{h_f} \left(\|\llbracket \mathbf{n} \times \mathbf{u} \rrbracket\|_{L^2(f)}^2 + \|\llbracket \mathbf{n} \times \mathbf{p} \rrbracket\|_{L^2(f)}^2 \right) + \sum_{f \in \mathcal{F}_h^b} \frac{\mu}{h_f} \|\mathbf{n} \times \mathbf{u} - \mathbf{n} \times \mathbf{g}\|_{L^2(f)}^2, \end{aligned}$$

where μ is a positive parameter and will be specified later on. We note that in two dimensions the variable \mathbf{p} in (3) is scalar-valued and in three dimensions the variable \mathbf{p} is a vector in \mathbb{R}^3 . Then, we define two approximation spaces \mathbf{V}_h^m and Σ_h^m for the variables \mathbf{u} and \mathbf{p} , respectively,

$$\mathbf{V}_h^m := (V_h^m)^d, \quad \Sigma_h^m := (V_h^m)^{2d-3},$$

where V_h^m is the standard piecewise polynomial space,

$$V_h^m := \{v_h \in L^2(\Omega) \mid v_h|_K \in \mathbb{P}_m(K), \forall K \in \mathcal{T}_h\}.$$

Clearly, the functions in \mathbf{V}_h^m and Σ_h^m can be discontinuous across inter-element faces. We seek the numerical solution $(\mathbf{u}_h, \mathbf{p}_h) \in \mathbf{V}_h^m \times \Sigma_h^m$ by minimizing the functional (3) over the space $\mathbf{V}_h^m \times \Sigma_h^m$, which reads:

$$(4) \quad (\mathbf{u}_h, \mathbf{p}_h) = \arg \min_{(\mathbf{v}_h, \mathbf{q}_h) \in \mathbf{V}_h^m \times \Sigma_h^m} J_h(\mathbf{v}_h, \mathbf{q}_h).$$

To solve the minimization problem (4), we can write the corresponding Euler-Lagrange equation, which takes the form: find $(\mathbf{u}_h, \mathbf{p}_h) \in \mathbf{V}_h^m \times \Sigma_h^m$ such that

$$(5) \quad a_h(\mathbf{u}_h, \mathbf{p}_h; \mathbf{v}_h, \mathbf{q}_h) = l_h(\mathbf{v}_h, \mathbf{q}_h), \quad \forall (\mathbf{v}_h, \mathbf{q}_h) \in \mathbf{V}_h^m \times \Sigma_h^m,$$

where the bilinear form $a_h(\cdot; \cdot)$ and the linear form $l_h(\cdot)$ are defined as

$$\begin{aligned}
(6) \quad a_h(\mathbf{u}_h, \mathbf{p}_h; \mathbf{v}_h, \mathbf{q}_h) &:= \sum_{K \in \mathcal{T}_h} \int_K (\nabla \times \mathbf{p}_h - k\mathbf{u}_h) \cdot (\nabla \times \mathbf{q}_h - k\mathbf{v}_h) d\mathbf{x} \\
&+ \sum_{K \in \mathcal{T}_h} \int_K (\nabla \times \mathbf{u}_h - k\mathbf{p}_h) \cdot (\nabla \times \mathbf{v}_h - k\mathbf{q}_h) d\mathbf{x} \\
&+ \sum_{f \in \mathcal{F}_h^i} \frac{\mu}{h_f} \int_f [\mathbf{n} \times \mathbf{u}_h] \cdot [\mathbf{n} \times \mathbf{v}_h] ds \\
&+ \sum_{f \in \mathcal{F}_h^i} \frac{\mu}{h_f} \int_f [\mathbf{n} \times \mathbf{p}_h] \cdot [\mathbf{n} \times \mathbf{q}_h] ds \\
&+ \sum_{f \in \mathcal{F}_h^b} \frac{\mu}{h_f} \int_f (\mathbf{n} \times \mathbf{u}_h) \cdot (\mathbf{n} \times \mathbf{v}_h) ds,
\end{aligned}$$

and

$$\begin{aligned}
l_h(\mathbf{v}_h, \mathbf{q}_h) &:= - \sum_{K \in \mathcal{T}_h} \int_K \mathbf{f} \cdot \mathbf{v}_h d\mathbf{x} + \sum_{K \in \mathcal{T}_h} \int_K \nabla \times \mathbf{q}_h \cdot \tilde{\mathbf{f}} d\mathbf{x} \\
&+ \sum_{f \in \mathcal{F}_h^b} \frac{\mu}{h_f} \int_f \mathbf{n} \times \mathbf{v}_h \cdot \mathbf{g} ds.
\end{aligned}$$

Then we focus on the error estimate to the problem (5). To do so, we first define the spaces \mathbf{V}_h and Σ_h as

$$\mathbf{V}_h = \mathbf{V}_h^m + H_0(\text{curl}), \quad \Sigma_h = \Sigma_h^m + H(\text{curl}).$$

We introduce the following energy norms for both the spaces:

$$\|\mathbf{u}\|_{\mathbf{u}}^2 = \sum_{K \in \mathcal{T}_h} \left(\|\mathbf{u}\|_{L^2(K)}^2 + \|\nabla \times \mathbf{u}\|_{L^2(K)}^2 \right) + \sum_{f \in \mathcal{F}_h} \frac{1}{h_f} \|[\mathbf{n} \times \mathbf{u}]\|_{L^2(f)}^2, \quad \forall \mathbf{u} \in \mathbf{V}_h,$$

and

$$\|\mathbf{p}\|_{\mathbf{p}}^2 = \sum_{K \in \mathcal{T}_h} \left(\|\mathbf{p}\|_{L^2(K)}^2 + \|\nabla \times \mathbf{p}\|_{L^2(K)}^2 \right) + \sum_{f \in \mathcal{F}_h^i} \frac{1}{h_f} \|[\mathbf{n} \times \mathbf{p}]\|_{L^2(f)}^2, \quad \forall \mathbf{p} \in \Sigma_h,$$

and we define the energy norm $\|\cdot\|$ as

$$\|(\mathbf{u}, \mathbf{p})\|^2 = \|\mathbf{u}\|_{\mathbf{u}}^2 + \|\mathbf{p}\|_{\mathbf{p}}^2, \quad \forall (\mathbf{u}, \mathbf{p}) \in \mathbf{V}_h \times \Sigma_h.$$

It is easy to see that $\|\cdot\|_{\mathbf{u}}$ indeed defines a norm on \mathbf{V}_h and $\|\cdot\|_{\mathbf{p}}$ indeed defines a norm on Σ_h . As a result, $\|\cdot\|$ defines a norm on $\mathbf{V}_h \times \Sigma_h$. Then we state the continuity result of the bilinear form $a_h(\cdot; \cdot)$ with respect to the norm $\|\cdot\|$.

Lemma 1. *Let the bilinear form $a_h(\cdot; \cdot)$ be defined as (6) with any positive μ , there exists a constant C such that*

$$(7) \quad |a_h(\mathbf{u}, \mathbf{p}; \mathbf{v}, \mathbf{q})| \leq C \|(\mathbf{u}, \mathbf{p})\| \|(\mathbf{v}, \mathbf{q})\|,$$

for any $(\mathbf{u}, \mathbf{p}), (\mathbf{v}, \mathbf{q}) \in \mathbf{V}_h \times \Sigma_h$.

Proof. Using the Cauchy-Schwartz inequality, we have that

$$\begin{aligned} \sum_{K \in \mathcal{T}_h} \int_K k^2 \mathbf{u} \cdot \mathbf{v} dx &\leq k^2 \left(\sum_{K \in \mathcal{T}_h} \|\mathbf{u}\|_{L^2(K)}^2 \right)^{\frac{1}{2}} \left(\sum_{K \in \mathcal{T}_h} \|\mathbf{v}\|_{L^2(K)}^2 \right)^{\frac{1}{2}} \\ &\leq k^2 \|(\mathbf{u}, \mathbf{p})\| \|(\mathbf{v}, \mathbf{q})\|. \end{aligned}$$

Other terms that appear in the bilinear form (6) can be bounded similarly, which gives us the inequality (7) and completes the proof. \square

In order to prove the coercivity of the bilinear form $a_h(\cdot, \cdot)$, we require the following lemmas.

Lemma 2. *For any $\mathbf{u}_h \in \mathbf{V}_h^m$, there exists a piecewise polynomial $\mathbf{v}_h \in \mathbf{V}_h^m \cap H_0(\text{curl})$ such that*

$$\begin{aligned} \|\mathbf{u}_h - \mathbf{v}_h\|_{L^2(\Omega)}^2 &\leq C \sum_{f \in \mathcal{F}_h} h_f \|[\mathbf{n} \times \mathbf{u}_h]\|_{L^2(f)}^2, \\ (8) \quad \|\mathbf{u}_h - \mathbf{v}_h\|_{\mathbf{u}}^2 &\leq C \sum_{f \in \mathcal{F}_h} \frac{1}{h_f} \|[\mathbf{n} \times \mathbf{u}_h]\|_{L^2(f)}^2, \end{aligned}$$

and for any $\mathbf{p}_h \in \boldsymbol{\Sigma}_h^m$, there exists a piecewise polynomial $\mathbf{w}_h \in \boldsymbol{\Sigma}_h^m \cap H(\text{curl})$ such that

$$\begin{aligned} \|\mathbf{p}_h - \mathbf{w}_h\|_{L^2(\Omega)}^2 &\leq C \sum_{f \in \mathcal{F}_h^i} h_f \|[\mathbf{n} \times \mathbf{p}_h]\|_{L^2(f)}^2, \\ (9) \quad \|\mathbf{p}_h - \mathbf{w}_h\|_{\mathbf{p}}^2 &\leq C \sum_{f \in \mathcal{F}_h^i} \frac{1}{h_f} \|[\mathbf{n} \times \mathbf{p}_h]\|_{L^2(f)}^2. \end{aligned}$$

Proof. We prove this lemma by using the similar techniques as those in [15, 20, 22]. In two dimensions, \mathbf{p}_h is a scalar-valued piecewise polynomial function. For scalar-valued functions, the space $H(\text{curl})$ is equal to the space $H^1(\Omega)$. By [20, Theorem 2.1], there exists a piecewise polynomial $\mathbf{w}_h \in \boldsymbol{\Sigma}_h^m \cap H^1(\Omega)$ satisfying the estimate (9). For the vector-valued function \mathbf{u} , we will use Nédélec's elements of the second type in two dimensions to prove the result and the estimate (8). In three dimensions, \mathbf{u}_h and \mathbf{p}_h are both vector-valued piecewise polynomials and we will apply 3D Nédélec's elements of the second type to prove the two results. We primarily deduce that for the three-dimensional case and it is almost trivial to extend the proof to 2D for vector-valued functions.

We first give some properties about Nédélec's edge elements of the second type, which was introduced by Nédélec [28]. For a bounded domain D , we define the polynomial space $\mathbb{D}_l(D)$ as $\mathbb{D}_l(D) = \mathbb{P}_{k-1}(D)^d \oplus \tilde{\mathbb{P}}_{k-1}(D)\mathbf{x}$, where $\tilde{\mathbb{P}}_{k-1}(D)$ is the space of homogeneous polynomials of degree $k-1$. For a tetrahedral element K and a polynomial $\mathbf{v} \in \mathbb{P}(K)^d$, three types of moments (degrees of freedom) of the Nédélec's elements associated with

edges of K , faces of K and K itself are defined as follows,

$$\begin{aligned} M_K^e(\mathbf{t}) &= \left\{ \int_e (\mathbf{t} \cdot \boldsymbol{\tau}_e) q \, ds, \quad \forall q \in \mathbb{P}_m(e) \right\}, \quad \text{for any edge } e \in \partial K, \\ M_K^f(\mathbf{t}) &= \left\{ \frac{1}{|f|} \int_f \mathbf{t} \cdot \mathbf{q} \, ds, \quad \forall \mathbf{q} \in \mathbb{D}_{m-1}(f) \right\}, \quad \text{for any face } f \in \partial K, \\ M_K^b(\mathbf{t}) &= \left\{ \int_K \mathbf{t} \cdot \mathbf{q} \, dx, \quad \forall \mathbf{q} \in \mathbb{D}_{m-2}(K) \right\}, \end{aligned}$$

where $\boldsymbol{\tau}_e$ denotes the unit vector along the edge. Further, for any polynomial $\mathbf{t} \in \mathbb{P}_m(K)^d$, we define $t_{K,e}^i \in M_K^e(\mathbf{t})$, $t_{K,f}^i \in M_K^f(\mathbf{t})$ and $t_{K,b}^i \in M_K^b(\mathbf{t})$ as the corresponding moments of \mathbf{t} . We let $\{\phi_{K,e}^i\}$, $\{\phi_{K,f}^i\}$, $\{\phi_{K,b}^i\}$ are the Lagrange bases of the space $\mathbb{P}_m(K)^d$ with respect to the moments, respectively. Then, any polynomial $\mathbf{v} \in \mathbb{P}_m(K)^d$ can be uniquely expressed as

$$\mathbf{v} = \sum_{e \in \mathcal{E}(K)} \sum_{i=1}^{N_e} v_{K,e}^i \phi_{K,e}^i + \sum_{f \in \mathcal{F}(K)} \sum_{i=1}^{N_f} v_{K,f}^i \phi_{K,f}^i + \sum_{i=1}^{N_b} v_{K,b}^i \phi_{K,b}^i,$$

where $\mathcal{E}(K)$ and $\mathcal{F}(K)$ are the sets of edges and faces of the element K , respectively.

Then we state the following estimates. For an element K and any polynomial $\mathbf{v} \in \mathbb{P}_m(K)^d$, there exists a constant C such that

$$(10) \quad h_K^{-2} \|\mathbf{v}\|_{L^2(K)}^2 + \|\nabla \times \mathbf{v}\|_{L^2(K)}^2 \leq Ch_K^{-1} \left(\sum_{e \in \mathcal{E}(K)} \sum_{i=1}^{N_e} (v_{K,e}^i)^2 + \sum_{f \in \mathcal{F}(K)} \sum_{i=1}^{N_f} (v_{K,f}^i)^2 + \sum_{i=1}^{N_b} (v_{K,b}^i)^2 \right).$$

For an interior face $f \in \mathcal{F}_h^i$ shared by K_1 and K_2 . For any polynomial $\mathbf{v}_1 \in \mathbb{P}_m(K_1)^d$ and $\mathbf{v}_2 \in \mathbb{P}_m(K_2)^d$, there exists a constant C such that

$$(11) \quad \sum_{i=1}^{N_f} (v_{K_1,f}^i - v_{K_2,f}^i)^2 + \sum_{e \in \mathcal{E}(f)} \sum_{i=1}^{N_e} (v_{K_1,e}^i - v_{K_2,e}^i)^2 \leq C \int_f |\mathbf{n}_f \times (\mathbf{v}_1 - \mathbf{v}_2)|^2 \, ds,$$

where $\mathcal{E}(f)$ is the set of edges belonging to the face f and \mathbf{n}_f is the unit outward normal on f . For a boundary face f , we let K be the element such that $f \in \partial K$. Then, there exists a constant C such that

$$(12) \quad \sum_{i=1}^{N_f} (v_{K,f}^i)^2 + \sum_{e \in \mathcal{E}(f)} \sum_{i=1}^{N_e} (v_{K,e}^i)^2 \leq C \int_f |\mathbf{n}_f \times \mathbf{v}|^2 \, ds.$$

The estimates (10), (11) and (12) are obtained from the equivalence of norms over finite dimensional spaces and the scaling argument. We refer to [15, 26] for the details of their proofs.

Then we construct two new piecewise polynomials $\mathbf{w}_h \in \boldsymbol{\Sigma}_h^m \cap H(\text{curl})$ and $\mathbf{v}_h \in \mathbf{V}_h^m \cap H_0(\text{curl})$ satisfying the estimates (9) and (8), respectively. To construct \mathbf{w}_h , for the element

K , we define its moments $\{w_{K,e}^i\}$, $\{w_{K,f}^i\}$ and $\{w_{K,b}^i\}$ as follows,

$$(13) \quad w_{K,e}^i = \sum_{\tilde{K} \in N(e)} \frac{1}{|N(e)|} p_{\tilde{K},e}^i, \quad \forall e \in \mathcal{E}_h, \quad 1 \leq i \leq N_e,$$

and

$$(14) \quad w_{K,f}^i = \sum_{\tilde{K} \in N(f)} \frac{1}{|N(f)|} p_{\tilde{K},f}^i, \quad \forall f \in \mathcal{F}_h, \quad 1 \leq i \leq N_f,$$

and

$$w_{K,b}^i = p_{K,b}^i, \quad 1 \leq i \leq N_b.$$

Here we let $N(e)$, $N(f)$ be the sets of elements that contain the edge e and the face f , respectively, and we denote their cardinalities as $|N(e)|$ and $|N(f)|$. Clearly, the above moments will yield a piecewise polynomial $\mathbf{w}_h \in \Sigma_h^m \cap H(\text{curl})$. Then we focus on the error between \mathbf{w}_h and \mathbf{p}_h . From (10), we deduce that

$$(15) \quad h_K^{\alpha-1} \|\mathbf{p}_h - \mathbf{w}_h\|_{L^2(K)}^2 + h_K^{\alpha+1} \|\nabla \times (\mathbf{p}_h - \mathbf{w}_h)\|_{L^2(K)}^2 \leq Ch_K^\alpha \left(\sum_{e \in \mathcal{E}(K)} \sum_{i=1}^{N_e} (p_{K,e}^i - w_{K,e}^i)^2 + \sum_{f \in \mathcal{F}(K)} \sum_{i=1}^{N_f} (p_{K,f}^i - w_{K,f}^i)^2 \right), \quad \alpha = \pm 1,$$

on the element K . By (13), we only need to consider the error for the edge e which satisfies $|N(e)| \geq 2$. For such an edge e , we let e be shared by a sequence of elements $\{K_{e,1}, K_{e,2}, \dots, K_{e,|N(e)|}\}$ with $K_{e,1} = K$ and $K_{e,i}, K_{e,i+1}$ are two neighbouring elements. Then the edge e will be shared by $|N(e)| + 1$ faces, which are $\{f_{e,1}, f_{e,2}, f_{e,|N(e)|+1}\}$ where $f_{e,i}, f_{e,i+1}$ are the adjacent faces of the element $K_{e,i}$, and we further have that $f_{e,2}, \dots, f_{e,|N(e)|} \in \mathcal{F}_h^i$. Then from (10) and the mesh regularity, we deduce that

$$(16) \quad \begin{aligned} \sum_{i=1}^{N_e} h_K^\alpha (p_{K,e}^i - w_{K,e}^i)^2 &\leq C \sum_{j=2}^{|N(e)|} \sum_{i=1}^{N_e} h_K^\alpha (p_{K_{e,1},e}^i - w_{K_{e,j},e}^i)^2 \\ &\leq C \sum_{j=1}^{|N(e)|-1} \sum_{i=1}^{N_e} h_K^\alpha (p_{K_{e,j},e}^i - w_{K_{e,j+1},e}^i)^2 \\ &\leq C \sum_{j=2}^{|N(e)|} \int_{f_{e,j}} h_{f_{e,j}}^\alpha \|\llbracket \mathbf{n} \times \mathbf{p}_h \rrbracket\|^2 ds \\ &\leq C \sum_{f \in \mathcal{F}(e) \cap \mathcal{F}_h^i} h_f^\alpha \|\llbracket \mathbf{n} \times \mathbf{p}_h \rrbracket\|_{L^2(f)}^2, \end{aligned}$$

where $\mathcal{F}(e)$ are the set of faces that contain the edge e .

By (14), we consider the errors on interior faces, and from (11) we obtain that

$$(17) \quad \begin{aligned} \sum_{i=1}^{N_f} h_K^\alpha (p_{K,f}^i - w_{K,f}^i)^2 &\leq C \sum_{K' \in N(f)} \sum_{i=1}^{N_f} h_K^\alpha (p_{K,f}^i - p_{K',f}^i)^2 \\ &\leq Ch_f^\alpha \|[\mathbf{n} \times \mathbf{p}_h]\|_{L^2(f)}^2, \end{aligned}$$

for the face $f \in \mathcal{F}_h^i$. Combining the estimates (15), (16) and (17), and summing over all elements arrives at the estimate (9).

The construction of the piecewise polynomial \mathbf{v}_h is similar. We define its corresponding moments $\{v_{K,e}^i\}$, $\{v_{K,f}^i\}$ and $\{v_{K,b}^i\}$ as

$$v_{K,e}^i = \begin{cases} \sum_{\tilde{K} \in N(e)} \frac{1}{|N(e)|} u_{\tilde{K},e}^i, & \forall e \in \mathcal{E}_h^i, \\ 0, & \forall e \in \mathcal{E}_h^b, \end{cases}, \quad 1 \leq i \leq N_e,$$

and

$$v_{K,f}^i = \begin{cases} \sum_{\tilde{K} \in N(f)} \frac{1}{|N(f)|} u_{\tilde{K},f}^i, & \forall f \in \mathcal{F}_h^i, \\ 0, & \forall f \in \mathcal{F}_h^b, \end{cases}, \quad 1 \leq i \leq N_f,$$

and

$$v_{K,b}^i = u_{K,b}^i, \quad 1 \leq i \leq N_b.$$

The above moments obviously imply that $\mathbf{v}_h \in H_0(\text{curl})$. We note that the moments of \mathbf{v}_h and \mathbf{w}_h are only different on boundary edges and faces. Hence the estimates (17) and (16) also hold for \mathbf{v}_h on interior edges and faces. On the element K , we have that

$$\sum_{i=1}^{N_e} h_K^\alpha (u_{K,e}^i - v_{K,e}^i) \leq C \sum_{f \in \mathcal{F}(e)} h_f^\alpha \|[\mathbf{n} \times \mathbf{u}_h]\|_{L^2(f)}^2,$$

for an interior edge $e \in \mathcal{E}(K)$, and

$$\sum_{i=1}^{N_f} h_K^\alpha (u_{K,f}^i - v_{K,f}^i)^2 \leq Ch_f^\alpha \|[\mathbf{n} \times \mathbf{u}_h]\|_{L^2(f)}^2,$$

for an interior face $f \in \mathcal{F}(K)$. For boundary edges and faces, we directly apply the estimate (12) to obtain the analogous inequalities, which bring us that

$$\begin{aligned} &h_K^{\alpha-1} \|\mathbf{u}_h - \mathbf{v}_h\|_{L^2(K)}^2 + h_K^{\alpha+1} \|\nabla \times (\mathbf{u}_h - \mathbf{v}_h)\|_{L^2(K)}^2 \\ &\leq C \left(\sum_{e \in \mathcal{E}(K)} \sum_{f \in \mathcal{F}(e)} h_f^\alpha \|[\mathbf{n} \times \mathbf{u}_h]\|_{L^2(f)}^2 + \sum_{f \in \mathcal{F}(K)} h_f^\alpha \|[\mathbf{n} \times \mathbf{u}_h]\|_{L^2(f)}^2 \right), \quad \alpha = \pm 1. \end{aligned}$$

We finally arrive at the estimate (8) by summing over all elements. This completes the proof. \square

Lemma 3. *There exists a constant C such that*

$$(18) \quad \|\mathbf{u}\|_{\mathbf{u}} + \|\mathbf{p}\|_{\mathbf{p}} \leq C (\|\nabla \times \mathbf{u} - k\mathbf{p}\|_{L^2(\Omega)} + \|\nabla \times \mathbf{p} - k\mathbf{u}\|_{L^2(\Omega)}),$$

for any $\mathbf{u} \in \mathbf{V}_h^m \cap H_0(\text{curl})$ and any $\mathbf{p} \in \Sigma_h^m \cap H(\text{curl})$.

Proof. We let

$$\nabla \times \mathbf{u} - k\mathbf{p} = \mathbf{f}_1, \quad \nabla \times \mathbf{p} - k\mathbf{u} = \mathbf{f}_2.$$

For any $\boldsymbol{\psi} \in H_0(\text{curl})$, we have

$$(\nabla \times \mathbf{u}, \nabla \times \boldsymbol{\psi})_{L^2(\Omega)} - k(\mathbf{p}, \nabla \times \boldsymbol{\psi})_{L^2(\Omega)} = (\mathbf{f}_1, \nabla \times \boldsymbol{\psi})_{L^2(\Omega)},$$

and

$$(\nabla \times \mathbf{p}, \boldsymbol{\psi})_{L^2(\Omega)} - k(\mathbf{u}, \boldsymbol{\psi}) = (\mathbf{f}_2, \boldsymbol{\psi})_{L^2(\Omega)}.$$

Using the integration by parts to obtain that

$$(\nabla \times \mathbf{u}, \nabla \times \boldsymbol{\psi})_{L^2(\Omega)} - k^2(\mathbf{u}, \boldsymbol{\psi})_{L^2(\Omega)} = (\mathbf{f}_1, \nabla \times \boldsymbol{\psi})_{L^2(\Omega)} + k(\mathbf{f}_2, \boldsymbol{\psi})_{L^2(\Omega)}.$$

By [13, Theorem 5.2], we derive that

$$\begin{aligned} \|\mathbf{u}\|_{H(\text{curl})} &\leq C \sup_{\boldsymbol{\psi} \in H_0(\text{curl})} \frac{(\nabla \times \mathbf{u}, \nabla \times \boldsymbol{\psi})_{L^2(\Omega)} - k^2(\mathbf{u}, \boldsymbol{\psi})_{L^2(\Omega)}}{\|\boldsymbol{\psi}\|_{H(\text{curl})}} \\ &\leq C \sup_{\boldsymbol{\psi} \in H_0(\text{curl})} \frac{(\mathbf{f}_1, \nabla \times \boldsymbol{\psi})_{L^2(\Omega)} + k(\mathbf{f}_2, \boldsymbol{\psi})_{L^2(\Omega)}}{\|\boldsymbol{\psi}\|_{H(\text{curl})}} \\ &\leq C (\|\mathbf{f}_1\|_{L^2(\Omega)} + \|\mathbf{f}_2\|_{L^2(\Omega)}). \end{aligned}$$

Since $\mathbf{u} \in H_0(\text{curl})$, we have that $\|\mathbf{u}\|_{H(\text{curl})} = \|\mathbf{u}\|_{\mathbf{u}}$. Further, we deduce that

$$\begin{aligned} \|\mathbf{p}\|_{\mathbf{p}} &= \|\mathbf{p}\|_{H(\text{curl})} \leq C (\|\mathbf{p}\|_{L^2(\Omega)} + \|\nabla \times \mathbf{p}\|_{L^2(\Omega)}) \\ &\leq C (\|\mathbf{f}_1\|_{L^2(\Omega)} + \|\nabla \times \mathbf{u}\|_{L^2(\Omega)} + \|\mathbf{f}_2\|_{L^2(\Omega)} + \|\mathbf{u}\|_{L^2(\Omega)}) \\ &\leq C (\|\mathbf{f}_1\|_{L^2(\Omega)} + \|\mathbf{f}_2\|_{L^2(\Omega)}), \end{aligned}$$

which gives us the estimate (18) and completes the proof. \square

Now we are ready to state that the bilinear form $a_h(\cdot; \cdot)$ is coercive with respect to the energy norms.

Lemma 4. *Let the bilinear form $a_h(\cdot; \cdot)$ be defined as (6) with any positive μ , there exists a constant C such that*

$$(19) \quad a_h(\mathbf{u}_h, \mathbf{p}_h; \mathbf{u}_h, \mathbf{p}_h) \geq C \|(\mathbf{u}_h, \mathbf{p}_h)\|^2,$$

for any $(\mathbf{u}_h, \mathbf{p}_h) \in \mathbf{V}_h^m \times \boldsymbol{\Sigma}_h^m$.

Proof. Clearly, we have that

$$\begin{aligned} a_h(\mathbf{u}_h, \mathbf{p}_h; \mathbf{u}_h, \mathbf{p}_h) &= \sum_{K \in \mathcal{T}_h} \left(\|\nabla \times \mathbf{p}_h - k\mathbf{u}_h\|_{L^2(K)}^2 + \|\nabla \times \mathbf{u}_h - k\mathbf{p}_h\|_{L^2(K)}^2 \right) \\ &\quad + \sum_{f \in \mathcal{F}_h^i} \frac{\mu}{h_f} \left(\|[\mathbf{n} \times \mathbf{u}_h]\|_{L^2(f)}^2 + \|[\mathbf{n} \times \mathbf{p}_h]\|_{L^2(f)}^2 \right) + \sum_{f \in \mathcal{F}_h^b} \frac{\mu}{h_f} \|\mathbf{n} \times \mathbf{u}_h\|_{L^2(f)}^2. \end{aligned}$$

By Lemma 2, for \mathbf{u}_h and \mathbf{p}_h , there exists a polynomial $\mathbf{v}_h \in \mathbf{V}_h^m \cap H_0(\text{curl})$ such that

$$\|\mathbf{u}_h - \mathbf{v}_h\|_{\mathbf{u}}^2 \leq C \sum_{f \in \mathcal{F}_h} \frac{1}{h_f} \|[\mathbf{n} \times \mathbf{u}_h]\|_{L^2(f)}^2 \leq C a_h(\mathbf{u}_h, \mathbf{p}_h; \mathbf{u}_h, \mathbf{p}_h),$$

and there exists a polynomial $\mathbf{q}_h \in \Sigma_h^m \cap H(\text{curl})$ such that

$$\|\mathbf{p}_h - \mathbf{q}_h\|_{\mathbf{p}}^2 \leq C \sum_{f \in \mathcal{F}_h^i} \frac{1}{h_f} \|[\mathbf{n} \times \mathbf{p}_h]\|_{L^2(f)}^2 \leq C a_h(\mathbf{u}_h, \mathbf{p}_h; \mathbf{u}_h, \mathbf{p}_h).$$

Hence,

$$\begin{aligned} \|(\mathbf{u}_h, \mathbf{p}_h)\|^2 &\leq C (\|(\mathbf{u}_h - \mathbf{v}_h, \mathbf{p}_h - \mathbf{q}_h)\|^2 + \|(\mathbf{v}_h, \mathbf{q}_h)\|^2) \\ &\leq C (a_h(\mathbf{u}_h, \mathbf{p}_h; \mathbf{u}_h, \mathbf{p}_h) + \|(\mathbf{v}_h, \mathbf{q}_h)\|^2). \end{aligned}$$

By Lemma 3, we get that

$$\begin{aligned} \|(\mathbf{v}_h, \mathbf{q}_h)\|^2 &\leq (\|\mathbf{v}_h\|_{\mathbf{u}} + \|\mathbf{q}_h\|_{\mathbf{p}})^2 \\ &\leq C (\|\nabla \times \mathbf{v}_h - \mathbf{q}_h\|_{L^2(\Omega)} + \|\nabla \times \mathbf{q}_h - \mathbf{v}_h\|_{L^2(\Omega)})^2. \end{aligned}$$

We apply the triangle inequality to derive that

$$\begin{aligned} \|\nabla \times \mathbf{v}_h - \mathbf{q}_h\|_{L^2(\Omega)}^2 &\leq C \left(\|\nabla \times \mathbf{u}_h - \mathbf{p}_h\|_{L^2(\mathcal{T}_h)}^2 + \|\nabla \times (\mathbf{u}_h - \mathbf{v}_h)\|_{L^2(\mathcal{T}_h)}^2 + \|\mathbf{p}_h - \mathbf{q}_h\|_{L^2(\Omega)}^2 \right) \\ &\leq C \left(\|\nabla \times \mathbf{u}_h - \mathbf{p}_h\|_{L^2(\mathcal{T}_h)}^2 + \|\mathbf{u}_h - \mathbf{v}_h\|_{\mathbf{u}}^2 + \|\mathbf{p}_h - \mathbf{q}_h\|_{\mathbf{p}}^2 \right) \\ &\leq C a_h(\mathbf{u}_h, \mathbf{p}_h; \mathbf{u}_h, \mathbf{p}_h). \end{aligned}$$

Similarly, we have that

$$\|\nabla \times \mathbf{q}_h - \mathbf{v}_h\|_{L^2(\Omega)}^2 \leq C a_h(\mathbf{u}_h, \mathbf{p}_h; \mathbf{u}_h, \mathbf{p}_h).$$

Combining all inequalities above, we arrive at

$$a_h(\mathbf{u}_h, \mathbf{p}_h; \mathbf{u}_h, \mathbf{p}_h) \geq C \|(\mathbf{u}_h, \mathbf{p}_h)\|^2,$$

which gives the estimate (19) and completes the proof. \square

Remark 1. We note that here we have attained the coercivity result of the bilinear form $a_h(\cdot; \cdot)$. This property allows us to derive the error estimate from the Lax-Milgram framework instead of using the Gårding-type inequality. In addition, the estimate (19) holds true unconditionally without any constraint on the mesh size.

Then we state the Galerkin orthogonality of the bilinear form $a_h(\cdot; \cdot)$.

Lemma 5. Let the bilinear form $a_h(\cdot; \cdot)$ be defined as (6) with any positive μ . Let $(\mathbf{u}, \mathbf{p}) \in H(\text{curl}) \times H(\text{curl})$ be the exact solution to (2), and let $(\mathbf{u}_h, \mathbf{p}_h) \in \mathbf{V}_h^m \times \Sigma_h^m$ be the solution to (5). Then, the following equation holds true

$$(20) \quad a_h(\mathbf{u} - \mathbf{u}_h, \mathbf{p} - \mathbf{p}_h; \mathbf{v}_h, \mathbf{q}_h) = 0,$$

for any $(\mathbf{v}_h, \mathbf{q}_h) \in \mathbf{V}_h^m \times \Sigma_h^m$.

Proof. The regularity of the exact solution (\mathbf{u}, \mathbf{p}) directly brings us that

$$[\mathbf{n} \times \mathbf{u}] = \mathbf{0}, \quad [\mathbf{n} \times \mathbf{p}] = \mathbf{0}, \quad \text{on } \forall f \in \mathcal{F}_h^i.$$

Hence,

$$\begin{aligned}
a_h(\mathbf{u} - \mathbf{u}_h, \mathbf{p} - \mathbf{p}_h; \mathbf{v}_h, \mathbf{q}_h) &= \sum_{K \in \mathcal{T}_h} \int_K (\nabla \times (\mathbf{p} - \mathbf{p}_h) - k(\mathbf{u} - \mathbf{u}_h)) \cdot (\nabla \times \mathbf{q}_h - k\mathbf{v}_h) d\mathbf{x} \\
&+ \sum_{K \in \mathcal{T}_h} \int_K (\nabla \times (\mathbf{u} - \mathbf{u}_h) - k(\mathbf{p} - \mathbf{p}_h)) \cdot (\nabla \times \mathbf{v}_h - k\mathbf{q}_h) d\mathbf{x} \\
&+ \sum_{f \in \mathcal{F}_h^i} \frac{\mu}{h_f} \int_f [\mathbf{n} \times \mathbf{u}_h] \cdot [\mathbf{n} \times \mathbf{v}_h] ds + \sum_{f \in \mathcal{F}_h^i} \frac{\mu}{h_f} \int_f [\mathbf{n} \times \mathbf{p}_h] \cdot [\mathbf{n} \times \mathbf{q}_h] ds \\
&+ \sum_{f \in \mathcal{F}_h^b} \frac{\mu}{h_f} \int_f (\mathbf{n} \times (\mathbf{u} - \mathbf{u}_h)) \cdot (\mathbf{n} \times \mathbf{v}_h) ds \\
&= \sum_{K \in \mathcal{T}_h} \int_K \tilde{\mathbf{f}} \cdot (\nabla \times \mathbf{q}_h - k\mathbf{v}_h) d\mathbf{x} + \sum_{f \in \mathcal{F}_h^b} \frac{\mu}{h_f} \int_f \mathbf{g} \cdot (\mathbf{n} \times \mathbf{v}_h) ds - a_h(\mathbf{u}_h, \mathbf{p}_h; \mathbf{v}_h, \mathbf{q}_h) \\
&= l_h(\mathbf{v}_h, \mathbf{q}_h) - a_h(\mathbf{u}_h, \mathbf{p}_h; \mathbf{v}_h, \mathbf{q}_h) \\
&= 0,
\end{aligned}$$

which yields the equation (20) and completes the proof. \square

Finally, we state the *a priori* error estimate of the method proposed in this section under the energy norm $\|\cdot\|$.

Theorem 1. *Let (\mathbf{u}, \mathbf{p}) be the exact solution to (2), which admits the following regularity,*

$$\begin{aligned}
(\mathbf{u}, \mathbf{p}) &\in H^{m+1}(\Omega)^d \times H^{m+1}(\Omega)^{2d-3}, \\
(\nabla \times \mathbf{u}, \nabla \times \mathbf{p}) &\in H^{m+1}(\Omega)^{2d-3} \times H^{m+1}(\Omega)^d,
\end{aligned}$$

and let $(\mathbf{u}_h, \mathbf{p}_h) \in \mathbf{V}_h^m \times \Sigma_h^m$ be the numerical solution to (5), and let the bilinear form $a_h(\cdot; \cdot)$ be defined as (6) with any positive μ . Then there exists a constant C such that

$$(21) \quad \begin{aligned}
&\|(\mathbf{u} - \mathbf{u}_h, \mathbf{p} - \mathbf{p}_h)\| \leq \\
&Ch^m (\|\mathbf{u}\|_{H^{m+1}(\Omega)} + \|\nabla \times \mathbf{u}\|_{H^{m+1}(\Omega)} + \|\mathbf{p}\|_{H^{m+1}(\Omega)} + \|\nabla \times \mathbf{p}\|_{H^{m+1}(\Omega)}).
\end{aligned}$$

Proof. By Lemma 5, we have that

$$a_h(\mathbf{u} - \mathbf{u}_h, \mathbf{p} - \mathbf{p}_h; \mathbf{v}_h, \mathbf{q}_h) = 0, \quad \forall (\mathbf{v}_h, \mathbf{q}_h) \in \mathbf{V}_h^m \times \Sigma_h^m,$$

Together with Lemma 1 and Lemma 4, we obtain that

$$\begin{aligned}
\|(\mathbf{u}_h - \mathbf{v}_h, \mathbf{p}_h - \mathbf{q}_h)\|^2 &\leq Ca_h(\mathbf{u}_h - \mathbf{v}_h, \mathbf{p}_h - \mathbf{q}_h; \mathbf{u}_h - \mathbf{v}_h, \mathbf{p}_h - \mathbf{q}_h) \\
&= Ca_h(\mathbf{u} - \mathbf{v}_h, \mathbf{p} - \mathbf{q}_h; \mathbf{u}_h - \mathbf{v}_h, \mathbf{p}_h - \mathbf{q}_h) \\
&\leq C \|(\mathbf{u} - \mathbf{v}_h, \mathbf{p} - \mathbf{q}_h)\| \|(\mathbf{u}_h - \mathbf{v}_h, \mathbf{p}_h - \mathbf{q}_h)\|,
\end{aligned}$$

for any $(\mathbf{v}_h, \mathbf{q}_h) \in \mathbf{V}_h^m \times \Sigma_h^m$. We eliminate the term $\|(\mathbf{u} - \mathbf{v}_h, \mathbf{p} - \mathbf{q}_h)\|$ on both sides and apply the triangle inequality to get that

$$(22) \quad \|(\mathbf{u} - \mathbf{u}_h, \mathbf{p} - \mathbf{p}_h)\| \leq C \inf_{(\mathbf{v}_h, \mathbf{q}_h) \in \mathbf{V}_h^m \times \Sigma_h^m} \|(\mathbf{u} - \mathbf{v}_h, \mathbf{p} - \mathbf{q}_h)\|.$$

We denote by $(\mathbf{u}_I = \Pi_N \mathbf{u}, \mathbf{p}_I = \Pi_N \mathbf{p}) \in \mathbf{V}_h^m \times \boldsymbol{\Sigma}_h^m$ the Nédélec interpolants of the second kind to the exact solution (\mathbf{u}, \mathbf{p}) . Using the interpolation estimate [26, Theorem 5.41] and the trace estimate, we arrive at

$$\begin{aligned} \|\mathbf{u} - \mathbf{u}_I\|_{\mathbf{u}} &\leq Ch^m (\|\mathbf{u}\|_{H^{m+1}(\Omega)} + \|\nabla \times \mathbf{u}\|_{H^{m+1}(\Omega)}), \\ \|\mathbf{p} - \mathbf{p}_I\|_{\mathbf{p}} &\leq Ch^m (\|\mathbf{p}\|_{H^{m+1}(\Omega)} + \|\nabla \times \mathbf{p}\|_{H^{m+1}(\Omega)}). \end{aligned}$$

Substituting the above two estimates into (22) implies the error estimate (21), which completes the proof. \square

Notice that the framework of the least squares finite element method has a natural mesh refinement indicator, which is exactly the least squares functional defined as (3). Therefore, we define an element indicator η_K for the element K as

$$\begin{aligned} \eta_K^2 &:= \|\nabla \times \mathbf{p}_h - k\mathbf{u}_h - \tilde{\mathbf{f}}\|_{L^2(K)}^2 + \|\nabla \times \mathbf{u}_h - k\mathbf{p}_h\|_{L^2(K)}^2 \\ &\quad + \sum_{f \in \mathcal{F}_h^i \cap \mathcal{F}(K)} \frac{1}{h_f} \left(\|\llbracket \mathbf{n} \times \mathbf{u}_h \rrbracket\|_{L^2(f)}^2 + \|\llbracket \mathbf{n} \times \mathbf{p}_h \rrbracket\|_{L^2(f)}^2 \right) \\ &\quad + \sum_{f \in \mathcal{F}_h^b \cap \mathcal{F}(K)} \frac{1}{h_f} \|\mathbf{n} \times \mathbf{u}_h - \mathbf{n} \times \mathbf{g}\|_{L^2(f)}^2. \end{aligned} \tag{23}$$

The adaptive procedure consists of loops of the standard form:

$$\text{Solve} \rightarrow \text{Estimate} \rightarrow \text{Mark} \rightarrow \text{Refine.}$$

Ultimately, we present the following adaptive algorithm for solving the time-harmonic Maxwell equations:

- Step 1 Given the initial mesh \mathcal{T}_0 and a positive parameter θ , and set the iteration number $l = 0$;
- Step 2 Solve the time-harmonic Maxwell equations on the mesh \mathcal{T}_l ;
- Step 3 Obtain the error indicator η_K for all $K \in \mathcal{T}_l$ with respect to the numerical solutions from the Step 2;
- Step 4 Find the minimal subset $\mathcal{M} \subset \mathcal{T}_l$ such that $\theta \sum_{K \in \mathcal{T}_l} \eta_K^2 \leq \sum_{K \in \mathcal{M}} \eta_K^2$ and mark all elements in \mathcal{M} .
- Step 5 Refine all marked elements to generate the next level mesh \mathcal{T}_{l+1} ;
- Step 6 If the stop criterion is not satisfied, then go to the Step 2 and set $l = l + 1$.

4. NUMERICAL RESULTS

Below we present several numerical examples in two dimensions and three dimensions to demonstrate the performance of the proposed method. In all these numerical experiments, the parameter μ in (3) is selected to be 1 and we adopt the BiCGstab solver together with the ILU preconditioner to solve the resulting linear algebraic system.

Example 1. For the first example, we consider a smooth problem defined on the unit square domain $\Omega = (0, 1)^2$. The exact solution to the time-harmonic Maxwell equations is given by the smooth field [15],

$$\mathbf{u}(x, y) = \begin{bmatrix} \sin(ky) \\ \sin(kx) \end{bmatrix},$$

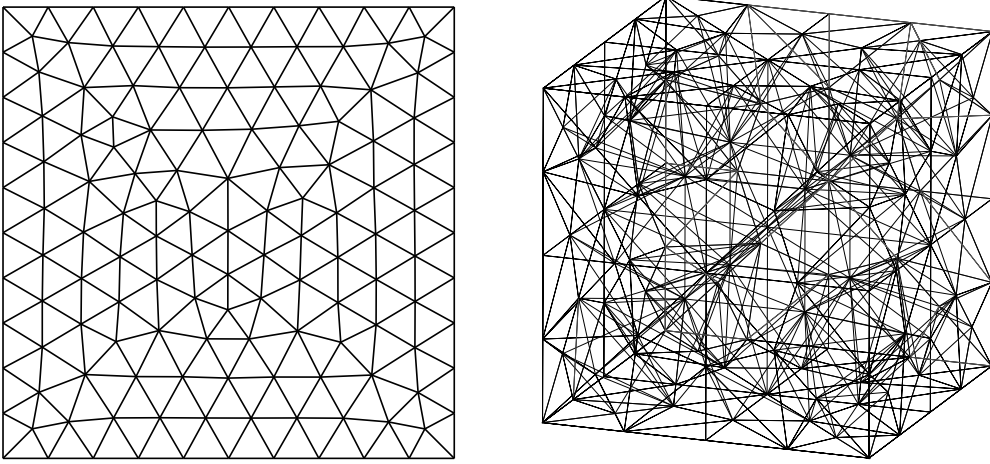


FIGURE 1. 2d triangular partition with $h = 1/10$ (left) / 3d tetrahedral partition with $h = 1/4$ (right).

and the source term \mathbf{f} and the non-homogeneous boundary data \mathbf{g} are chosen accordingly. We solve this problem on a series of shape-regular triangular meshes with the mesh size $h = 1/5, h = 1/10, \dots, 1/40$ (see Fig. 1). The convergence histories with the wave number $k = 1, 2, 8$ for the accuracy $1 \leq m \leq 3$ are presented in Tab. 1, Tab. 2 and Tab. 3, respectively. From the numerical errors, we observe that the error under the energy norm $\|(\mathbf{u} - \mathbf{u}_h, \mathbf{p} - \mathbf{p}_h)\|$ converges to zero with the optimal speed $O(h^m)$ as the mesh size approaches zero. In addition, for the L^2 errors, we can see that $\|\mathbf{u} - \mathbf{u}_h\|_{L^2(\Omega)}$ and $\|\mathbf{p} - \mathbf{p}_h\|_{L^2(\Omega)}$ converge to zero at the rate $O(h^m)$ and $O(h^{m+1})$, respectively, as the mesh is refined. As the wave number k increases, the errors in the approximation to the exact solution also become larger under all error measurements. Here, we note that the numerical results are consistent with those in [15]. In addition, all the computed convergence rates agree with the error estimate given in Theorem 1.

Example 2. In this test, we consider a three-dimensional problem in the unit cube $\Omega = (0, 1)^3$. We solve the test problem on a series of tetrahedral meshes with the resolution $h = 1/2, 1/4, 1/8, 1/16$, see Fig. 1. The analytical solution is selected as

$$\mathbf{u}(x, y, z) = \begin{bmatrix} \sin(ky) \sin(kz) \\ \sin(kx) \sin(kz) \\ \sin(kx) \sin(ky) \end{bmatrix},$$

and the data functions \mathbf{f} and \mathbf{g} are taken suitably. We use the approximation spaces $\mathbf{V}_h^m \times \boldsymbol{\Sigma}_h^m$ with $1 \leq m \leq 3$ to approximate \mathbf{u} and \mathbf{p} , respectively. The numerical results with the wave number $k = 1$ are shown in Tab. 4. We observe that under the energy norm $\|\cdot\|$ the numerical error tends to zero at the optimal speed $O(h^m)$ as the mesh size decreases to zero. For the L^2 errors, our method shows a sub-optimal convergence rates for both variables in three dimensions. We note that all numerical convergence orders are still consistent with the theoretical error estimate.

Example 3. In this test, we investigate the performance of the proposed method for dealing with the problem that involves a singularity at the corner. The domain Ω is the

m	mesh size	1/10	1/20	1/40	1/80	order
1	$\ (\mathbf{u} - \mathbf{u}_h, \mathbf{p} - \mathbf{p}_h)\ $	3.333e-2	1.667e-2	8.333e-3	4.166e-3	1.00
	$\ \mathbf{u} - \mathbf{u}_h\ _{L^2(\Omega)}$	1.638e-2	8.168e-3	4.073e-3	1.663e-2	1.00
	$\ \mathbf{p} - \mathbf{p}_h\ _{L^2(\Omega)}$	4.813e-4	1.208e-4	3.011e-5	7.512e-6	2.00
2	$\ (\mathbf{u} - \mathbf{u}_h, \mathbf{p} - \mathbf{p}_h)\ $	3.168e-4	7.922e-5	1.979e-5	4.950e-6	2.00
	$\ \mathbf{u} - \mathbf{u}_h\ _{L^2(\Omega)}$	8.417e-5	2.102e-5	5.250e-6	1.311e-6	2.00
	$\ \mathbf{p} - \mathbf{p}_h\ _{L^2(\Omega)}$	1.722e-6	2.156e-7	2.695e-8	3.369e-9	3.00
3	$\ (\mathbf{u} - \mathbf{u}_h, \mathbf{p} - \mathbf{p}_h)\ $	2.731e-6	3.402e-7	4.251e-8	5.312e-9	3.00
	$\ \mathbf{u} - \mathbf{u}_h\ _{L^2(\Omega)}$	1.122e-6	1.383e-7	1.722e-8	2.155e-9	3.00
	$\ \mathbf{p} - \mathbf{p}_h\ _{L^2(\Omega)}$	1.827e-8	1.140e-9	7.133e-11	4.472e-12	4.00

TABLE 1. Convergence history for Example 1 with $k = 1$.

m	h	1/10	1/20	1/40	1/80	order
1	$\ (\mathbf{u} - \mathbf{u}_h, \mathbf{p} - \mathbf{p}_h)\ $	1.342e-1	5.920e-2	2.846e-2	1.408e-2	1.02
	$\ \mathbf{u} - \mathbf{u}_h\ _{L^2(\Omega)}$	1.911e-2	4.873e-3	1.221e-3	3.049e-4	2.00
	$\ \mathbf{p} - \mathbf{p}_h\ _{L^2(\Omega)}$	9.042e-2	3.033e-2	1.191e-2	5.446e-2	1.03
2	$\ (\mathbf{u} - \mathbf{u}_h, \mathbf{p} - \mathbf{p}_h)\ $	2.493e-3	6.229e-4	1.556e-5	3.891e-5	2.00
	$\ \mathbf{u} - \mathbf{u}_h\ _{L^2(\Omega)}$	5.241e-4	1.307e-4	3.263e-5	8.149e-6	2.00
	$\ \mathbf{p} - \mathbf{p}_h\ _{L^2(\Omega)}$	2.223e-5	2.473e-6	2.999e-7	3.722e-8	3.01
3	$\ (\mathbf{u} - \mathbf{u}_h, \mathbf{p} - \mathbf{p}_h)\ $	3.68e-5	4.610e-6	5.769e-7	7.264e-8	3.00
	$\ \mathbf{u} - \mathbf{u}_h\ _{L^2(\Omega)}$	6.186e-6	7.759e-7	9.775e-8	1.228e-8	3.00
	$\ \mathbf{p} - \mathbf{p}_h\ _{L^2(\Omega)}$	2.055e-7	1.289e-8	8.080e-10	5.061e-11	4.00

TABLE 2. Convergence history for Example 1 with $k = 2$.

L-shaped domain $\Omega = (-1, 1)^2 \setminus [0, 1) \times (-1, 0]$ and we choose the exact solution, in polar coordinates (r, θ) , to be

$$(24) \quad \mathbf{u}(x, y) = \nabla((kr)^\alpha \sin(\alpha\theta)) + \begin{bmatrix} \sin(ky) \\ \sin(kx) \end{bmatrix},$$

with $\alpha = 2/3$. Notice that the function \mathbf{u} contains a singularity at $(0, 0)$ and \mathbf{u} only belongs to the space $H^{\alpha-\varepsilon}(\Omega)$ for arbitrary small ε . The mesh size of the coarsest triangular mesh is $h = 1/5$ and we uniformly refine the initial mesh for three times to solve the problem, see Fig. 2. We list the numerical errors under the L^2 norms against the mesh size in Tab. 5. From the table, we can see that the error $\|\mathbf{u} - \mathbf{u}_h\|_{L^2(\Omega)}$ converges to zero at the rate $O(h^\alpha)$ for all $1 \leq m \leq 3$, which is in agreement with the regularity of the function \mathbf{u} . For the variable p , the numerically detected convergence rate is about $O(h^{\alpha+2/3})$ in terms of the L^2 norm. The explanation of this convergence rate can be traced to the L-shaped

m	h	1/10	1/20	1/40	1/80	order
1	$\ (\mathbf{u} - \mathbf{u}_h, \mathbf{p} - \mathbf{p}_h)\ $	7.531e-0	4.277e-0	1.652e-0	5.121e-1	1.69
	$\ \mathbf{u} - \mathbf{u}_h\ _{L^2(\Omega)}$	6.482e-1	3.641e-1	1.382e-1	4.060e-2	1.76
	$\ \mathbf{p} - \mathbf{p}_h\ _{L^2(\Omega)}$	6.432e-1	3.566e-1	1.337e-1	3.848e-2	1.80
2	$\ (\mathbf{u} - \mathbf{u}_h, \mathbf{p} - \mathbf{p}_h)\ $	2.787e-1	4.213e-2	9.898e-3	2.462e-3	2.00
	$\ \mathbf{u} - \mathbf{u}_h\ _{L^2(\Omega)}$	2.079e-2	2.123e-3	4.336e-4	1.067e-4	2.02
	$\ \mathbf{p} - \mathbf{p}_h\ _{L^2(\Omega)}$	1.914e-2	1.246e-3	7.962e-5	5.359e-6	3.80
3	$\ (\mathbf{u} - \mathbf{u}_h, \mathbf{p} - \mathbf{p}_h)\ $	9.493e-3	1.182e-3	1.478e-4	1.848e-5	3.00
	$\ \mathbf{u} - \mathbf{u}_h\ _{L^2(\Omega)}$	3.841e-4	4.665e-5	5.875e-6	7.398e-7	3.00
	$\ \mathbf{p} - \mathbf{p}_h\ _{L^2(\Omega)}$	9.612e-5	3.724e-6	2.219e-7	1.386e-8	4.00

TABLE 3. Convergence history for Example 1 with $k = 8$.

m	h	1/2	1/4	1/8	1/16	order
1	$\ (\mathbf{u} - \mathbf{u}_h, \mathbf{p} - \mathbf{p}_h)\ $	2.410e-1	1.262e-1	6.433e-2	3.252e-1	1.00
	$\ \mathbf{u} - \mathbf{u}_h\ _{L^2(\Omega)}$	9.731e-2	5.958e-2	3.239e-2	1.663e-2	0.99
	$\ \mathbf{p} - \mathbf{p}_h\ _{L^2(\Omega)}$	3.343e-2	1.681e-2	8.051e-2	3.942e-2	1.00
2	$\ (\mathbf{u} - \mathbf{u}_h, \mathbf{p} - \mathbf{p}_h)\ $	3.638e-2	8.922e-3	2.221e-3	5.556e-4	2.00
	$\ \mathbf{u} - \mathbf{u}_h\ _{L^2(\Omega)}$	1.795e-2	4.381e-3	1.098e-3	2.773e-4	1.99
	$\ \mathbf{p} - \mathbf{p}_h\ _{L^2(\Omega)}$	7.575e-3	1.637e-3	3.767e-4	8.921e-5	2.05
3	$\ (\mathbf{u} - \mathbf{u}_h, \mathbf{p} - \mathbf{p}_h)\ $	1.876e-3	2.347e-4	2.953e-5	3.712e-6	3.00
	$\ \mathbf{u} - \mathbf{u}_h\ _{L^2(\Omega)}$	6.916e-4	9.972e-5	1.339e-5	1.733e-6	2.96
	$\ \mathbf{p} - \mathbf{p}_h\ _{L^2(\Omega)}$	6.650e-4	6.301e-5	6.513e-6	7.336e-7	3.15

TABLE 4. Convergence history for Example 2.

domain. We note that the observed convergence rates in this example are consistent with the results in [15, 29].

Example 4. In this test, we solve a low-regularity problem in three dimensions. We consider the unit cubic domain $\Omega = (0, 1)^3$ and we select the analytical solution \mathbf{u} as

$$\mathbf{u}(x, y, z) = \nabla(|\mathbf{x}|^\alpha) = \nabla((x^2 + y^2 + z^2)^{\alpha/2}),$$

with $\alpha = 1.2$. The source function \mathbf{f} and the inhomogeneous boundary data \mathbf{g} are selected accordingly, and the wave number k is set as 1. Clearly, \mathbf{u} contains a singularity near the corner $(0, 0, 0)$, which implies that the function \mathbf{u} lies in the space $H^{\alpha-1/2-\varepsilon}(\Omega)$ with any $\varepsilon > 0$. We adopt the same uniform meshes as in Example 2 to solve this problem. We list the errors in approximation to (\mathbf{u}, \mathbf{p}) under the L^2 norms in Tab. 6. The convergence rate of the L^2 error $\|\mathbf{p} - \mathbf{p}_h\|_{L^2(\Omega)}$ is numerically detected to be about 0.7 for all m . The rate is perfectly in agreement with the regularity of the function \mathbf{u} . For the L^2

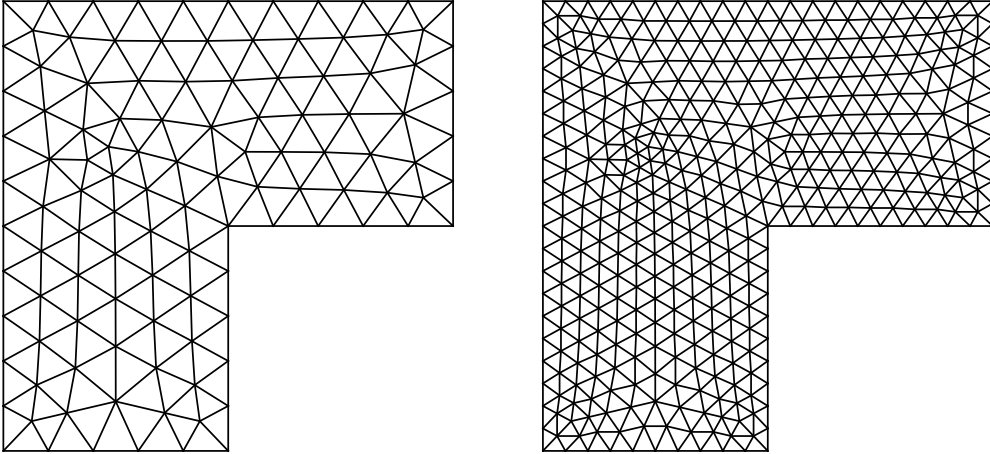


FIGURE 2. Triangular mesh for L-shaped domain with $h = 1/5$ (left) / $h = 1/10$ (right).

m	h	1/5	1/10	1/20	1/40	order
1	$\ \mathbf{u} - \mathbf{u}_h\ _{L^2(\Omega)}$	8.817e-2	5.112e-2	3.002e-2	1.801e-2	0.73
	$\ \mathbf{p} - \mathbf{p}_h\ _{L^2(\Omega)}$	2.115e-2	1.136e-2	5.039e-3	2.096e-3	1.26
2	$\ \mathbf{u} - \mathbf{u}_h\ _{L^2(\Omega)}$	4.001e-2	2.512e-2	1.581e-2	9.958e-3	0.67
	$\ \mathbf{p} - \mathbf{p}_h\ _{L^2(\Omega)}$	5.598e-3	2.070e-3	8.020e-4	3.163e-4	1.34
3	$\ \mathbf{u} - \mathbf{u}_h\ _{L^2(\Omega)}$	2.723e-2	1.718e-2	1.083e-2	6.820e-3	0.67
	$\ \mathbf{p} - \mathbf{p}_h\ _{L^2(\Omega)}$	8.478e-4	3.331e-4	1.309e-4	5.121e-5	1.35

TABLE 5. Convergence history for Example 3.

error $\|\mathbf{u} - \mathbf{u}_h\|_{L^2(\Omega)}$, the numerical convergence rate seems to be $O(h)$ higher than the variable \mathbf{p} , which is optimal as the mesh size tends to zero. We can not find this numerical phenomenon in the smooth case (see Tab. 4). The optimal L^2 convergence rate may depend on some properties of the exact solution and the mesh size, and we hope the reason can be clarified in our future research.

Example 5. In this example, we test our adaptive algorithm proposed in Section 3. We solve the low-regularity problem in Example 3. The domain is the L-shaped domain (see Fig. 4) and the exact solution is chosen as (24), which lies in the space $H^{2/3-\varepsilon}(\Omega)$ for any $\varepsilon > 0$. For the adaptive algorithm, we choose the parameter $\theta = 0.25$ and we use the longest-edge bisection algorithm to refine the mesh. We consider the linear accuracy $\mathbf{V}_h^1 \times \boldsymbol{\Sigma}_h^1$ to solve the problem. The convergence history under the L^2 norms for the adaptive refinement is displayed in Fig. 3. For this problem, as we demonstrated in Tab. 5, with the uniform refinement the L^2 errors tends to zero at the speed $O(N^{-0.67/2})$ and $O(N^{-1.35/2})$ for the variables \mathbf{u} and \mathbf{p} , respectively, where N is the number of elements in the partition. In Fig. 3, the convergence orders of the error $\|\mathbf{u} - \mathbf{u}_h\|_{L^2(\Omega)}$ and the error

m	h	1/2	1/4	1/8	1/16	order
1	$\ \mathbf{u} - \mathbf{u}_h\ _{L^2(\Omega)}$	4.082e-2	1.449e-2	4.836e-3	1.548e-3	1.65
	$\ \mathbf{p} - \mathbf{p}_h\ _{L^2(\Omega)}$	5.446e-3	3.746e-3	2.375e-3	1.475e-3	0.68
2	$\ \mathbf{u} - \mathbf{u}_h\ _{L^2(\Omega)}$	1.399e-2	4.375e-3	1.351e-3	4.158e-4	1.69
	$\ \mathbf{p} - \mathbf{p}_h\ _{L^2(\Omega)}$	2.996e-3	1.801e-3	1.112e-3	6.850e-4	0.70
3	$\ \mathbf{u} - \mathbf{u}_h\ _{L^2(\Omega)}$	5.846e-3	1.803e-3	5.553e-4	1.709e-4	1.69
	$\ \mathbf{p} - \mathbf{p}_h\ _{L^2(\Omega)}$	2.446e-3	1.478e-3	9.060e-4	5.578e-4	0.70

TABLE 6. Convergence history for Example 4.

$\|\mathbf{p} - \mathbf{p}_h\|_{L^2(\Omega)}$ approach zero seem to be about $O(N^{-1/2})$ and $O(N^{-1})$, respectively. We note that these two convergence rates match the convergence rates of the smooth case in Example 1. Moreover, we depict the triangular mesh after 10 adaptive steps in Fig. 4. Obviously, the refinement is pronounced around the corner $(0, 0)$ where the exact solution contains a singularity.

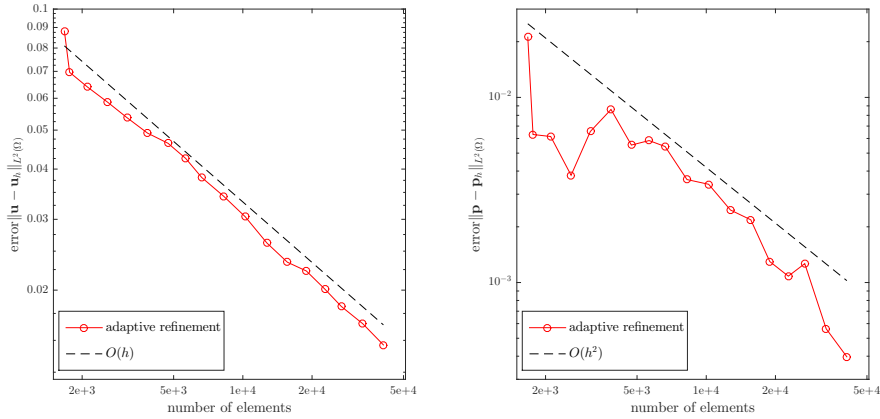


FIGURE 3. Convergence history for Example 5.

5. CONCLUSIONS

We proposed a discontinuous least squares finite element method for the time-harmonic Maxwell equations. Using discontinuous elements, we designed a least squares functional with the weak imposition of the tangential continuity on the interior faces. The convergence rates were derived with respect to the energy norm and the L^2 norm. Particularly, it was proved that our method is stable without any constraint on the mesh size. Numerical results in two dimensions and three dimensions illustrated the accuracy of our method.

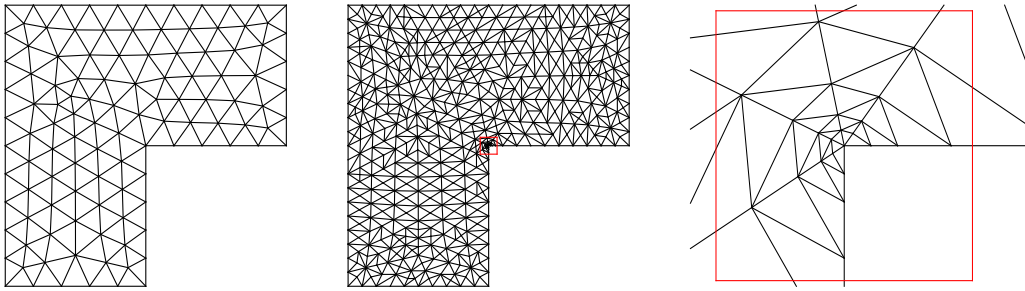


FIGURE 4. Initial mesh (left) / the triangular mesh after 10 adaptive refinement steps (middle) / the elements around the corner $(0,0)$ (right).

ACKNOWLEDGEMENTS

This research was supported by the Science Challenge Project (No. TZ2016002) and the National Science Foundation in China (No. 11971041).

REFERENCES

1. D. N. Arnold, F. Brezzi, B. Cockburn, and L. D. Marini, *Unified analysis of discontinuous Galerkin methods for elliptic problems*, SIAM J. Numer. Anal. **39** (2001/02), no. 5, 1749–1779.
2. Rickard Bensow and Mats G. Larson, *Discontinuous least-squares finite element method for the div-curl problem*, Numer. Math. **101** (2005), no. 4, 601–617.
3. Rickard E. Bensow and Mats G. Larson, *Discontinuous/continuous least-squares finite element methods for elliptic problems*, Math. Models Methods Appl. Sci. **15** (2005), no. 6, 825–842.
4. Pavel Bochev, James Lai, and Luke Olson, *A locally conservative, discontinuous least-squares finite element method for the Stokes equations*, Internat. J. Numer. Methods Fluids **68** (2012), no. 6, 782–804.
5. ———, *A non-conforming least-squares finite element method for incompressible fluid flow problems*, Internat. J. Numer. Methods Fluids **72** (2013), no. 3, 375–402.
6. Pavel B. Bochev and Max D. Gunzburger, *Finite element methods of least-squares type*, SIAM Rev. **40** (1998), no. 4, 789–837.
7. J. H. Bramble, T. V. Kolev, and J. E. Pasciak, *A least-squares approximation method for the time-harmonic Maxwell equations*, J. Numer. Math. **13** (2005), no. 4, 237–263.
8. James H. Bramble, Tzanio V. Kolev, and Joseph E. Pasciak, *The approximation of the Maxwell eigenvalue problem using a least-squares method*, Math. Comp. **74** (2005), no. 252, 1575–1598.
9. Susanne C. Brenner, Fengyan Li, and Li-Yeng Sung, *A locally divergence-free nonconforming finite element method for the time-harmonic Maxwell equations*, Math. Comp. **76** (2007), no. 258, 573–595.
10. Gang Chen, Jintao Cui, and Liwei Xu, *Analysis of a hybridizable discontinuous Galerkin method for the Maxwell operator*, ESAIM Math. Model. Numer. Anal. **53** (2019), no. 1, 301–324.
11. Zhiming Chen, Long Wang, and Weiyang Zheng, *An adaptive multilevel method for time-harmonic Maxwell equations with singularities*, SIAM J. Sci. Comput. **29** (2007), no. 1, 118–138.
12. Xiaobing Feng and Haijun Wu, *An absolutely stable discontinuous Galerkin method for the indefinite time-harmonic Maxwell equations with large wave number*, SIAM J. Numer. Anal. **52** (2014), no. 5, 2356–2380.
13. R. Hiptmair, *Finite elements in computational electromagnetism*, Acta Numer. **11** (2002), 237–339.
14. Ralf Hiptmair, Andrea Moiola, and Ilaria Perugia, *Stability results for the time-harmonic Maxwell equations with impedance boundary conditions*, Math. Models Methods Appl. Sci. **21** (2011), no. 11, 2263–2287.
15. Paul Houston, Ilaria Perugia, Anna Schneebeli, and Dominik Schötzau, *Interior penalty method for the indefinite time-harmonic Maxwell equations*, Numer. Math. **100** (2005), no. 3, 485–518.

16. Qiya Hu and Rongrong Song, *A variant of the plane wave least squares method for the time-harmonic Maxwell's equations*, ESAIM Math. Model. Numer. Anal. **53** (2019), no. 1, 85–103.
17. Qiya Hu and Long Yuan, *A plane-wave least-squares method for time-harmonic Maxwell's equations in absorbing media*, SIAM J. Sci. Comput. **36** (2014), no. 4, A1937–A1959.
18. J. Jagalur-Mohan, G. Feijóo, and A. Oberai, *A Galerkin least squares method for time harmonic Maxwell equations using Nédélec elements*, J. Comput. Phys. **235** (2013), 67–81.
19. Xue Jiang, Linbo Zhang, and Weiyang Zheng, *Adaptive hp-finite element computations for time-harmonic Maxwell's equations*, Commun. Comput. Phys. **13** (2013), no. 2, 559–582.
20. Ohannes A. Karakashian and Frederic Pascal, *Convergence of adaptive discontinuous Galerkin approximations of second-order elliptic problems*, SIAM J. Numer. Anal. **45** (2007), no. 2, 641–665.
21. Peijun Li, Gaofeng Zheng, and Weiyang Zheng, *Maxwell's equations in an unbounded structure*, Math. Methods Appl. Sci. **40** (2017), no. 3, 573–588.
22. Ruo Li and Fanyi Yang, *A sequential least squares method for elliptic equations in non-divergence form*, arXiv:1906.03754 (2019).
23. ———, *A least squares method for linear elasticity using a patch reconstructed space*, Comput. Methods Appl. Mech. Engrg. **363** (2020), no. 1.
24. ———, *A sequential least squares method for Poisson equation using a patch reconstructed space*, SIAM J. Numer. Anal. **58** (2020), no. 1, 353–374.
25. Peipei Lu, Huangxin Chen, and Weifeng Qiu, *An absolutely stable hp-HDG method for the time-harmonic Maxwell equations with high wave number*, Math. Comp. **86** (2017), no. 306, 1553–1577.
26. Peter Monk, *Finite element methods for Maxwell's equations*, Numerical Mathematics and Scientific Computation, Oxford University Press, New York, 2003.
27. J.-C. Nédélec, *Mixed finite elements in \mathbf{R}^3* , Numer. Math. **35** (1980), no. 3, 315–341.
28. ———, *A new family of mixed finite elements in \mathbf{R}^3* , Numer. Math. **50** (1986), no. 1, 57–81.
29. N. C. Nguyen, J. Peraire, and B. Cockburn, *Hybridizable discontinuous Galerkin methods for the time-harmonic Maxwell's equations*, J. Comput. Phys. **230** (2011), no. 19, 7151–7175.
30. I. Perugia, D. Schötzau, and P. Monk, *Stabilized interior penalty methods for the time-harmonic Maxwell equations*, Comput. Methods Appl. Mech. Engrg. **191** (2002), no. 41-42, 4675–4697.
31. Ilaria Perugia and Dominik Schötzau, *The hp-local discontinuous Galerkin method for low-frequency time-harmonic Maxwell equations*, Math. Comp. **72** (2003), no. 243, 1179–1214.
32. D. Sármany, F. Izsák, and J. J. W. van der Vegt, *Optimal penalty parameters for symmetric discontinuous Galerkin discretisations of the time-harmonic Maxwell equations*, J. Sci. Comput. **44** (2010), no. 3, 219–254.

CAPT, LMAM AND SCHOOL OF MATHEMATICAL SCIENCES, PEKING UNIVERSITY, BEIJING 100871, P.R. CHINA

E-mail address: rli@math.pku.edu.cn

SCHOOL OF MATHEMATICAL SCIENCES, PEKING UNIVERSITY, BEIJING 100871, P.R. CHINA

E-mail address: qc_liu@pku.edu.cn

SCHOOL OF MATHEMATICAL SCIENCES, PEKING UNIVERSITY, BEIJING 100871, P.R. CHINA

E-mail address: yangfanyi@pku.edu.cn